

ELECTRONIC SUPPLEMENTARY INFORMATION

A novel dimethylformamide (DMF) free bar-cast method to deposit organolead perovskite thin films with improved stability

Eurig W. Jones^a, Peter J. Holliman^{a*}, Arthur Connell^a, Matthew L. Davies^b, Jenny Baker^b, Robert J. Hobbs^a, Sanjay Ghosh^a, Leo Furnell^a, Rosie Anthony^a, Cameron Pleydell-Pearce^b

^a School of Chemistry, Bangor University, Bangor, Gwynedd LL57 2UW UK

^b SPECIFIC, Swansea University, Swansea, SA1 8EN UK

*Corresponding author email address: p.j.holliman@bangor.ac.uk

The paper describes a solvent-free approach to synthesizing organolead perovskites by using solid state reactions to coat perovskite crystals (i.e. powder) onto Al₂O₃ nanoparticles, followed by their suspension *via* addition of terpineol “solvent” (or dispersion medium) affording colloidal perovskite inks. Using these inks, we have bar cast photoactive perovskite thin films which are significantly more stable to humidity than solution processed films. This new method also avoids the use of toxic dimethylformamide (DMF) solvent. This ESI includes details of the methods used and data not shown in the manuscript.

1.0 Experimental

All chemicals were supplied by Aldrich and used as supplied unless otherwise stated.

CH₃NH₃PbI₂Cl perovskite ink

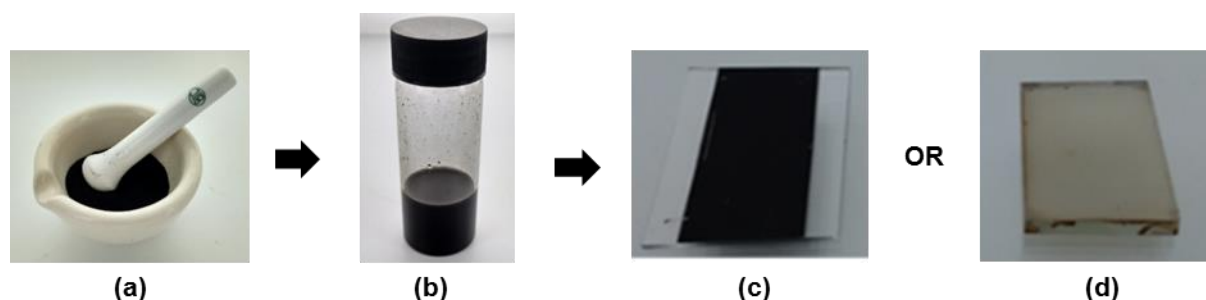
Methyl ammonium iodide (MAI) CH₃NH₃I was synthesised by reacting methylamine and hydroiodic acid in a 1:2 ratio. This was filtered and washed with diethyl ether before the solvent was removed by rotary evaporation affording MAI powder. Solvent-free deposition of perovskite thin films was achieved by:-

1. PbI₂ (1.0g) was ground in an agate pestle and mortar in a fume hood with Al₂O₃ (0.4g, mean particle size 13nm) leading to *ca.* 13% Al₂O₃ wt/wt loading when the CH₃NH₃I is added in. These were ground together until no further colour change was observed. Relative humidity was typically ≤40%.
2. Addition of CH₃NH₃I to the mix and mixing for a further 5 min, observing a colour change, nearly instantly, showing that the crystallization occurs very quickly, and affords nanoparticle perovskite crystals. Typical quantities when mixing were 1.679g CH₃NH₃I and 1.0g PbI₂, for CH₃NH₃PbI₃; 0.22g CH₃NH₃Br : 0.72g PbBr₂ for CH₃NH₃PbBr₃; 0.839g CH₃NH₃I and 0.5g PbCl₂ for CH₃NH₃PbI₂Cl

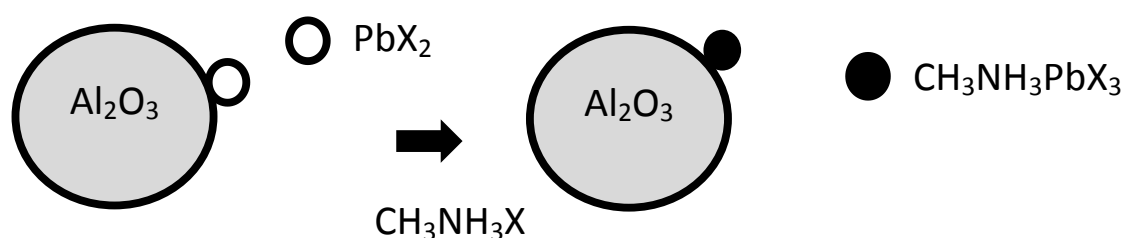
It should be noted here that initial mixtures were typically 3:1 CH₃NH₃X:PbX₂ (where X = halide) to mimic solution synthesis but it was quickly found that 1:1 molar mixtures worked best for these solid state reactions.

3. The resulting perovskite:alumina powder was suspended in α -terpineol (1.5ml, Aldrich) by mixing for 24h followed by sonication for 12h to ensure de-agglomeration (ESI Fig. 1b).
4. In a fume hood, perovskite ink was deposited onto borosilicate glass in a uniform line in front of a bar coater (RK Print K101 Control Coater). The ink was then automatically cast to produce a uniform film.

- For the photoluminescence studies, a blocking layer (*ca.* 80nm) was first deposited onto the glass substrate before the perovskite ink was bar coated. To do this, blocking layer solution was spin coated onto the substrate at 500rpm for 10s, 3000rpm for 60s and then 500rpm for 10s followed by sintering at 10°C/min to 500°C for 1h. Two blocking layers solutions were used; either Solaronix BL/SP or a freshly prepared in-house blocking layer solution. The latter was prepared by mixing equal volumes of a 0.5mM titanium isopropoxide solution in ethanol and a 40mM HCl solution in ethanol.
- The deposited films were then sintered from ambient to 70°C over a 15min ramp followed by a 10min dwell and then a 5 min ramp to 120°C followed by a 40min dwell. Finally, the films were cooled back to room temperature.



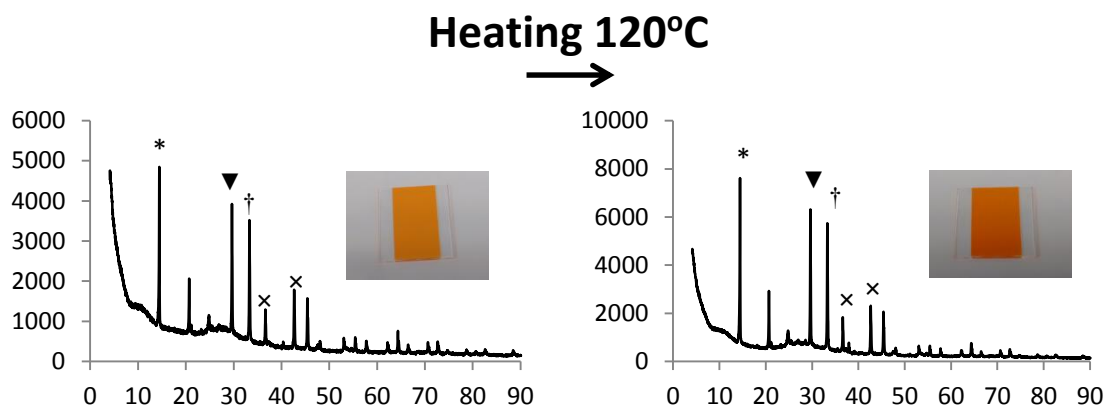
ESI Fig. 1 (a) Solvent-free, solid-state grinding reaction to synthesize organolead perovskite, (b) $\text{CH}_3\text{NH}_3\text{PbI}_3:\text{Al}_2\text{O}_3$ perovskite ink, (c) the resulting bar-cast perovskite film after 24h atmospheric exposure and (d) a spin coated, solution-processed perovskite film after 24h atmospheric exposure.



ESI Fig. 2 Schematic showing proposed outcome of initial grinding of PbX_2 X = halide with Al_2O_3 particles followed by addition of methylammonium halide.

2.0 Films produced from $\text{CH}_3\text{NH}_3\text{PbBr}_3:\text{Al}_2\text{O}_3$ ink

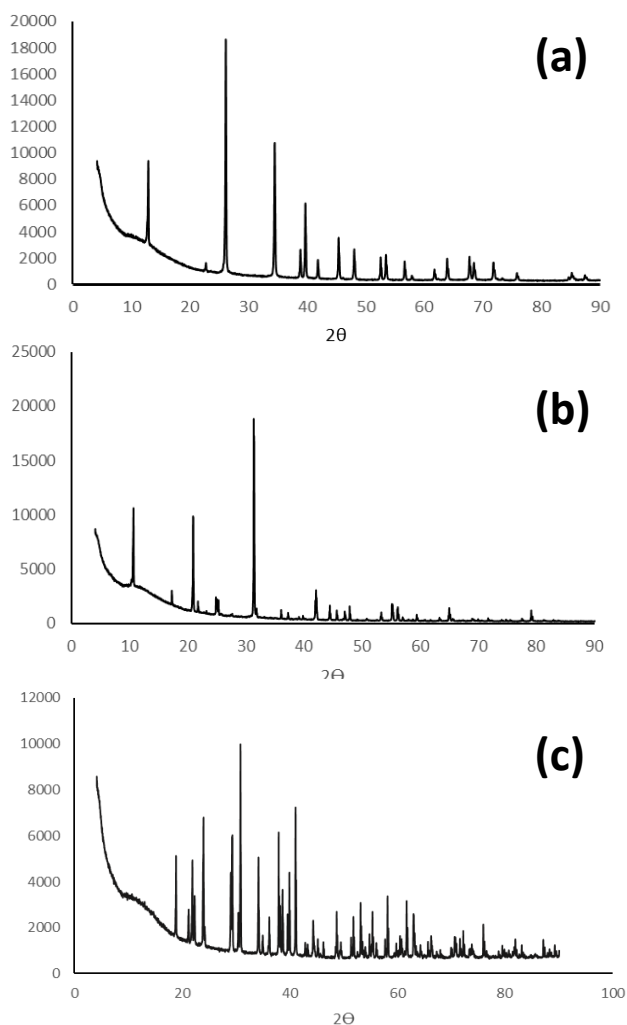
Alumina-based inks of the organolead tribromide perovskite ($\text{CH}_3\text{NH}_3\text{PbBr}_3:\text{Al}_2\text{O}_3$) have also been studied. Interestingly, as the methylammonium bromide and lead bromide are ground together, a colour change to orange begins to occur showing that the tribromide perovskite begins to crystallize at room temperature. The XRD data in ESI Fig. 3 confirms this but also show that the intensity of the diffraction peaks for the perovskite increase after sintering; e.g. the (110) line increases from 5000cps to 8000cps showing that crystallisation continues during annealing. This is interesting because the majority of Pb-based perovskites require heating to crystallise¹. Whilst this is not a problem for laboratory devices, it may be for scaled manufacturing because prolonged heating requires long processing ovens.



ESI Fig. 3 XRD patterns of films produced from $\text{CH}_3\text{NH}_3\text{PbBr}_3:\text{Al}_2\text{O}_3$ ink (left) before and (right) after sintering along with (inset) photographs showing colour of the sintered films. The main $\text{CH}_3\text{NH}_3\text{PbBr}_3$ perovskite diffraction lines are labelled as * (110), ▽ (220), † (310) along with × for the main Al_2O_3 diffraction lines.

3.0 Perovskite Raw Materials

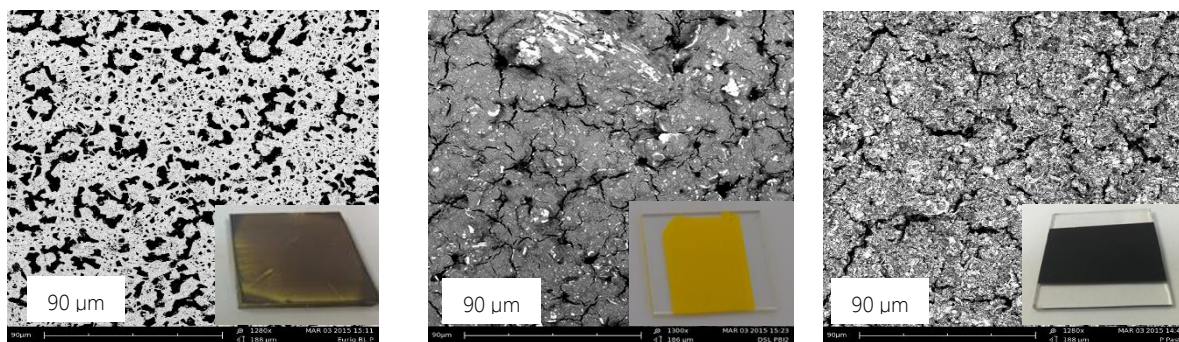
ESI Fig. 4 shows XRD data for the perovskite raw materials (lead halides and $\text{CH}_3\text{NH}_3\text{I}$).



ESI Fig. 4 X-ray diffraction pattern of (a) PbI_2 powder (99.9% purity), (b) in house synthesized $\text{CH}_3\text{NH}_3\text{I}$ and (c) PbBr_2 (99.9% purity)

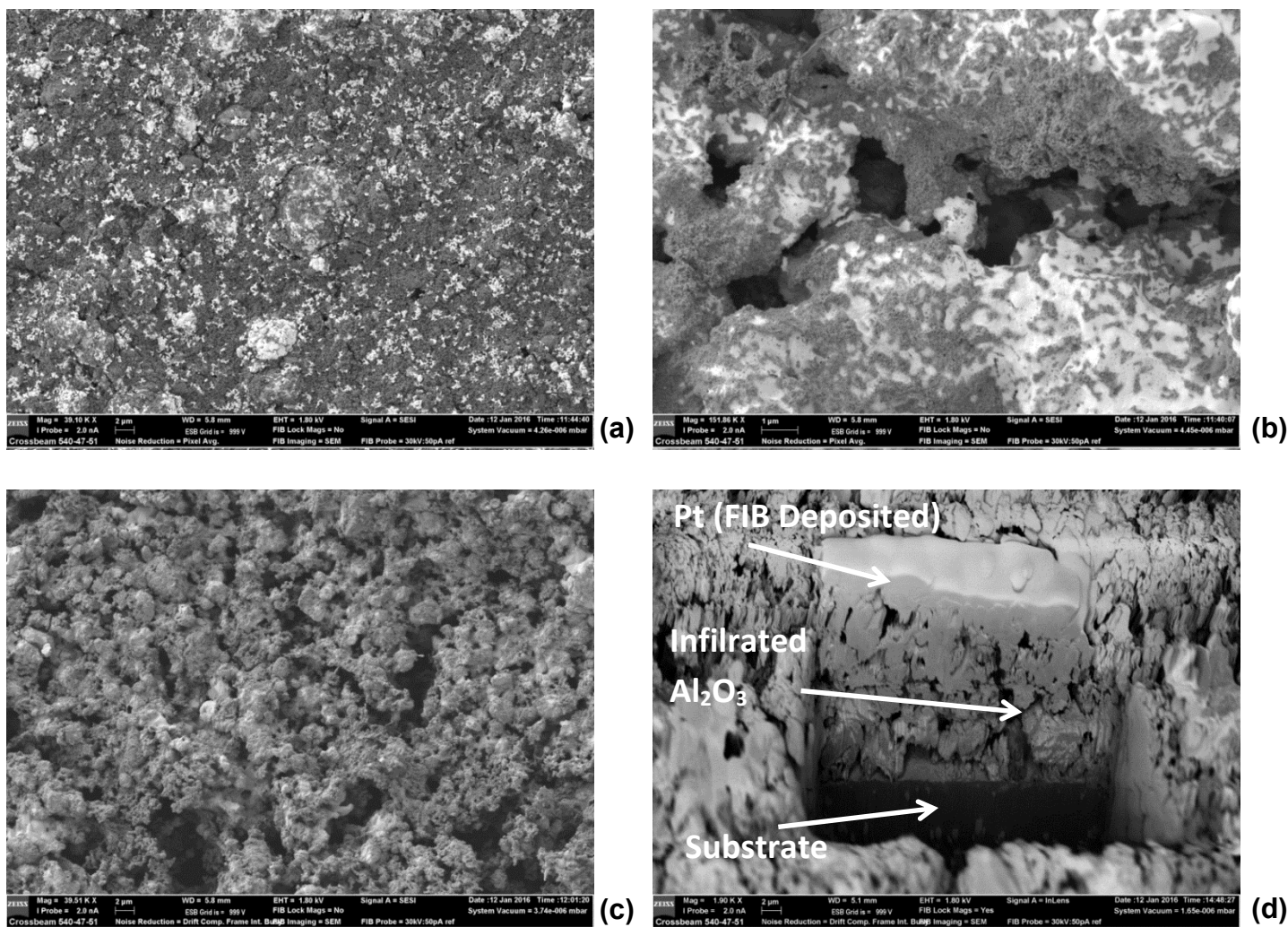
4.0 Scanning Electron Microscopy (SEM)

A Phenom desktop SEM was used to analyse the morphology and surface coverage of blade cast inks to compare with spin coated, solution processed perovskite films (ESI Fig. 5). The spin coated film (left) shows a thin film of perovskite crystals with dark voids between them. This film (inset) is black with yellowing at the edges indicating the film is beginning to degrade. By comparison, the blade coated inks (middle and right) show thicker, mesoporous films in line with the presence of Al_2O_3 scaffold. The middle image shows the result of PbI_2 and Al_2O_3 . The absence of two phases suggests that the PbI_2 coats the Al_2O_3 surface which is confirmed by the homogeneous yellow colour of the film (inset). The micrograph on the right shows the film which results from the perovskite ink which is produced after the addition of $\text{CH}_3\text{NH}_3\text{I}$ to the $\text{PbI}_2:\text{Al}_2\text{O}_3$ ink followed by grinding. The SEM data show a clear change to the surface of the Al_2O_3 scaffold with perovskite crystallites apparent. This $\text{CH}_3\text{NH}_3\text{PbI}_3$ perovskite phase is further evidenced by the colour change to a black film (inset).

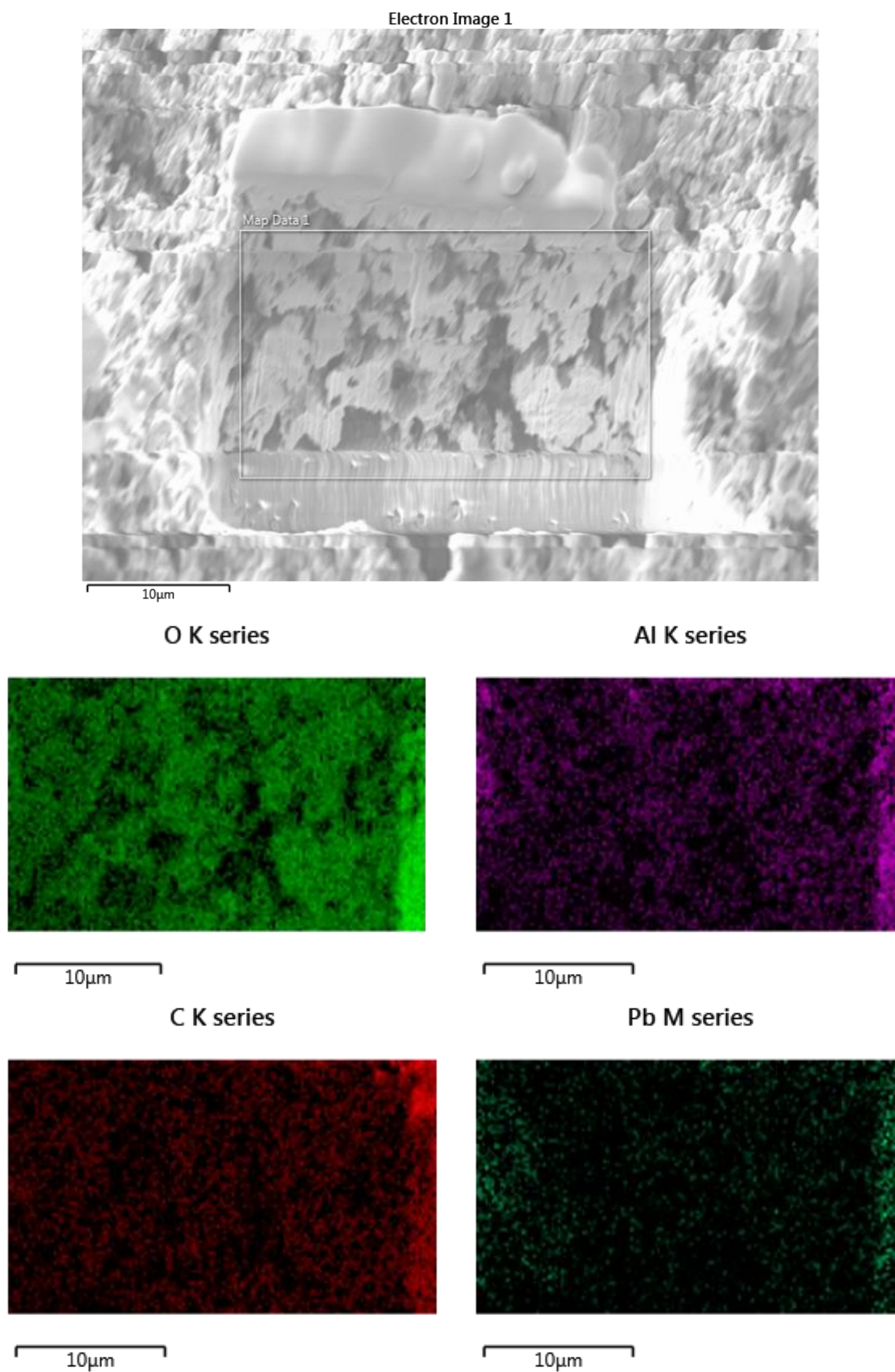


ESI Fig. 5 SEM images at 1300x magnification of films produced from (left) spin coated, solution processed perovskite, (middle) ground $\text{PbI}_2 + \text{Al}_2\text{O}_3$ nano-powders suspended in terpineol to create a PbI_2 ink and (right) $\text{CH}_3\text{NH}_3\text{PbI}_3:\text{Al}_2\text{O}_3$ terpineol ink.

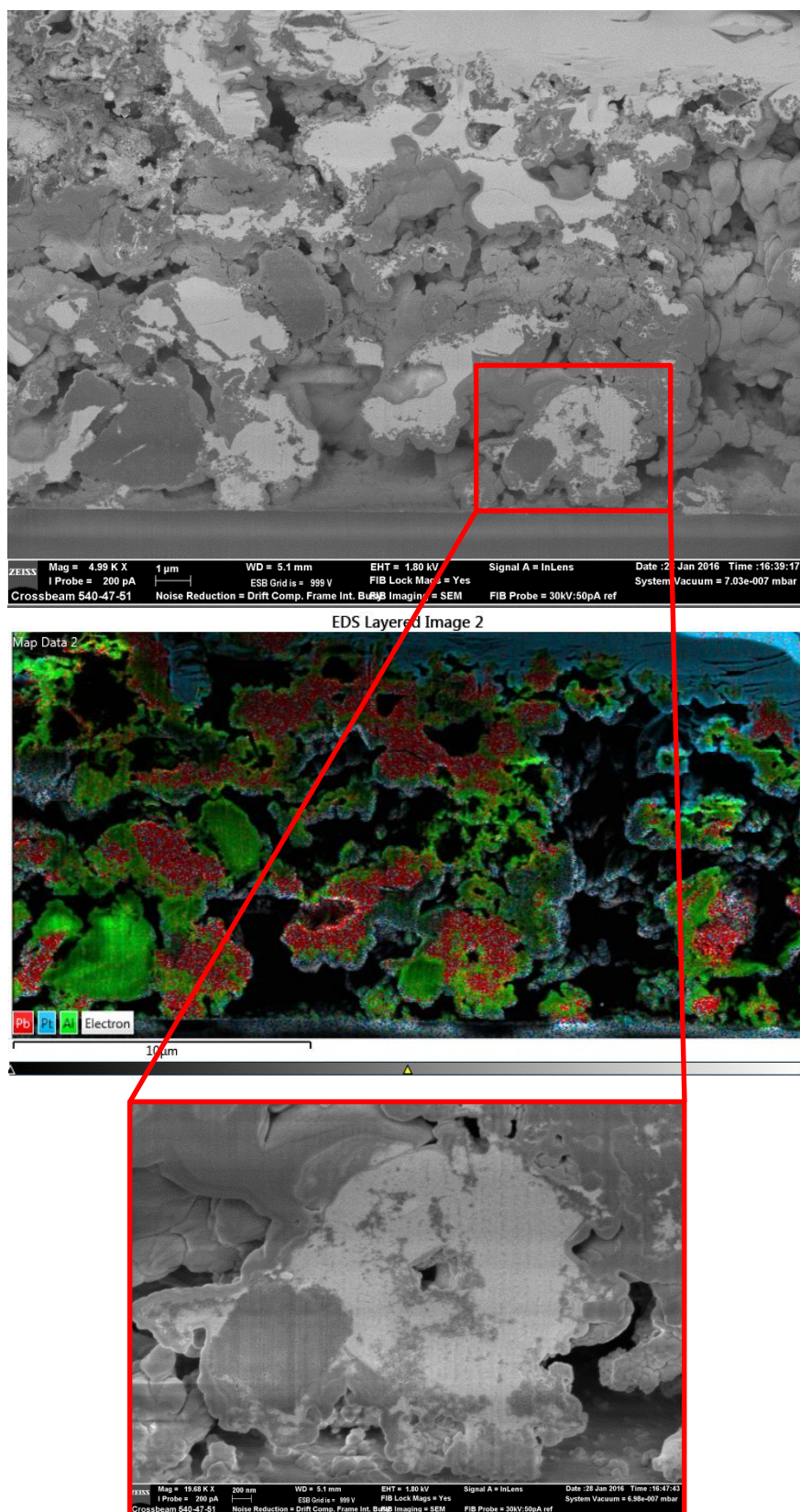
ESI Fig. 6 shows high resolution SEM images of perovskite ink films studied using a Zeiss Crossbeam 540 SEM with Gemini2 column. ESI Fig. 6a shows a plan view of a $\text{CH}_3\text{NH}_3\text{PbBr}_3:\text{Al}_2\text{O}_3$ ink film showing a smooth surface. The image has been produced by mixing back scattered (BSE) and secondary electron (SE) signals producing topological images where the heavier elements of the lead halide perovskite phase appear lighter in intensity and the Al_2O_3 appears darker. The images suggest that perovskite coats the Al_2O_3 in the films at a macro scale (in line with the higher intensity PL data for this sample) but with a less even coverage at a 100-200nm scale. The data for the $\text{CH}_3\text{NH}_3\text{PbI}_{3-x}\text{Cl}_x:\text{Al}_2\text{O}_3$ ink film (ESI Fig. 6b) show a rougher surface with larger agglomerations (*ca.* 10µm). The contrast in between lighter and darker areas suggests an uneven coverage of converted perovskite on the Al_2O_3 surface. The $\text{CH}_3\text{NH}_3\text{PbI}_3:\text{Al}_2\text{O}_3$ ink film data (ESI Figs. 6c, 7, 8) show a film which is rougher than the tri-bromide film but smoother than the mixed halide. Again there are darker and lighter areas which suggests incomplete perovskite coverage. Focussed ion beam cross-section of this film (ESI Fig. 6d, 7, 8) reveals densely packed Al_2O_3 particles with uneven perovskite surface coverage and some voids (essentially similar to the morphology of the film surface). EDS (ESI Fig. 7, 8) shows intense O and Al signals for Al_2O_3 . Signals for C and a weaker Pb signal confirm $\text{CH}_3\text{NH}_3\text{PbI}_3$ is present. The weaker Pb signal may suggest either incomplete surface coverage of perovskite or that the Pb M-edge was used to minimise accelerating voltage to minimise film damage. Film thickness is estimated to be 10-15µm which is thicker than the optimum for perovskite device films which are typically < 2µm.



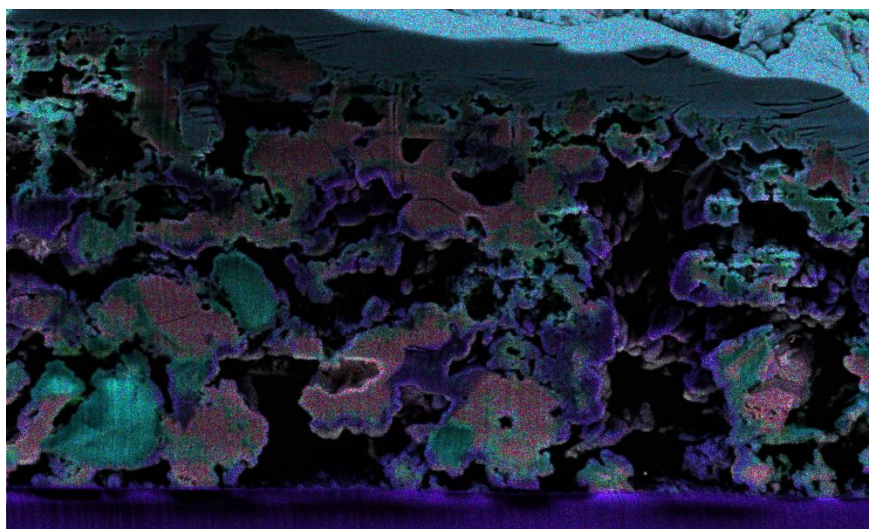
ESI Fig. 6 High resolution SEM images of surface topography with elemental contrast of annealed films of perovskite inks for (a) $\text{CH}_3\text{NH}_3\text{PbBr}_3:\text{Al}_2\text{O}_3$, (b) $\text{CH}_3\text{NH}_3\text{PbI}_{3-x}\text{Cl}_x:\text{Al}_2\text{O}_3$, and (c) $\text{CH}_3\text{NH}_3\text{PbI}_3:\text{Al}_2\text{O}_3$ and (d) cross-section of focussed ion beam (FIB) etched film of $\text{CH}_3\text{NH}_3\text{PbI}_3:\text{Al}_2\text{O}_3$ ink



ESI Fig. 7 Cross-section of focussed ion beam (FIB) etched film of $\text{CH}_3\text{NH}_3\text{PbI}_3:\text{Al}_2\text{O}_3$ ink and associated element maps from energy dispersive spectroscopy (EDS)



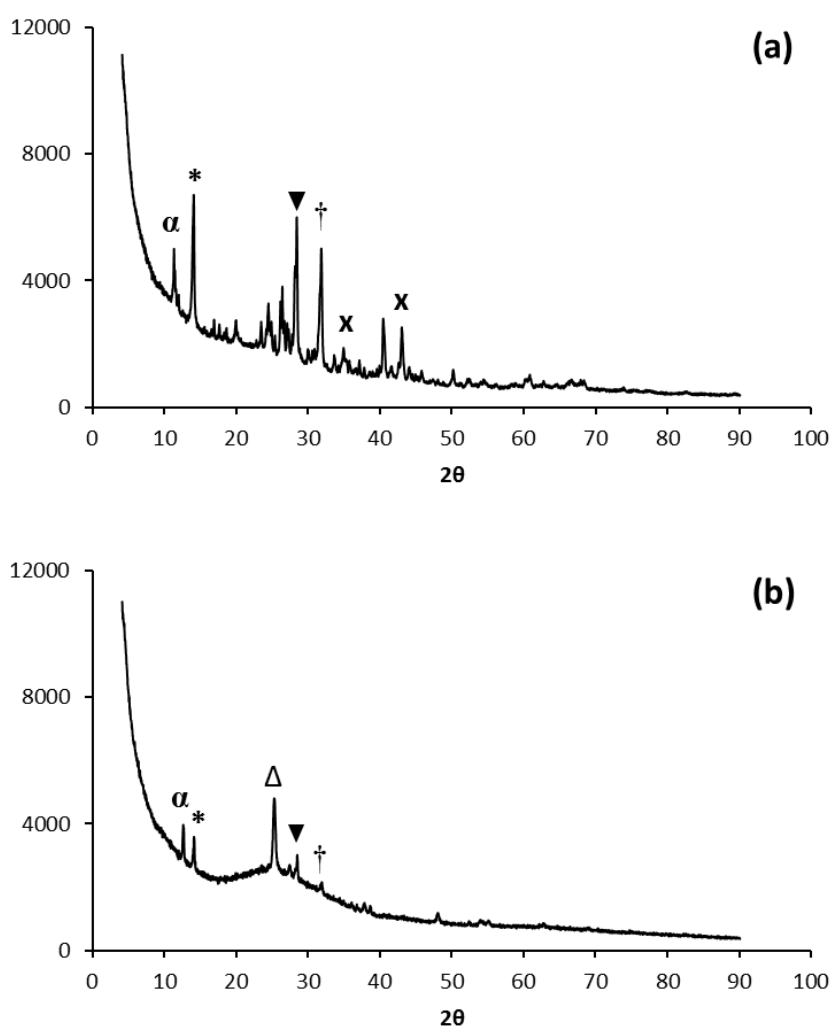
ESI Fig. 8a FIB etched cross-section of different region of film from $\text{CH}_3\text{NH}_3\text{PbI}_3:\text{Al}_2\text{O}_3$ ink (top), corresponding EDS element map showing uneven Pb coverage on Al_2O_3 (middle) and high magnification image of the film cross-section (bottom). Pb rich areas appear lighter.



ESI Fig. 8b EDS map of FIB etched cross-section of different region of film from $\text{CH}_3\text{NH}_3\text{PbI}_3:\text{Al}_2\text{O}_3$ ink (same area as ESI Fig. 8a). In this image, the purple areas denote silicon which is either from the glass substrate (at the bottom of the image) or is an artefact of the section preparation whereby glass has been re-deposited onto the sample during FIB etching.

5.0 Perovskite Film Lifetime Studies

ESI Fig. 9 shows X-ray diffraction data for organolead perovskite films produced using either alumina or titania as the scaffold material. In each case, the films have been left exposed to ambient conditions for 1500 hours. Both XRD patterns display a degradation and reduction in intensity of perovskite peaks compared to Fig. 2 of paper and also show a more prominent, PbI_2 peak (labelled α) indicating that some degradation has taken place. However, the data clearly show more intense perovskite diffraction line for the film produced from the alumina-based ink in line with the greater stability we have observed for these films both visually and by UV-visible spectroscopy. By comparison, the titania-based film shows only very weak intensity peaks for a perovskite phase indicating that most of this material has decomposed.

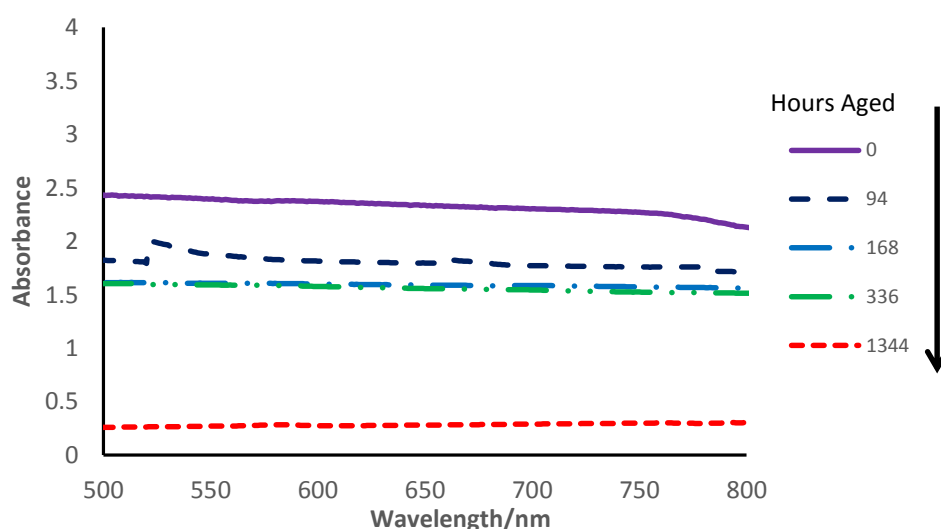


ESI Fig. 9 X-ray diffraction patterns of organolead perovskite films produced from either (a) alumina-based ink or (b) titania-based ink. Perovskite diffraction lines are labelled as * (110), ∇ (220), \dagger (310) whilst α is for PbI_2 , \times is for Al_2O_3 and Δ is or (101) TiO_2 diffraction lines.

5.1 UV-visible spectroscopy of perovskite film lifetimes

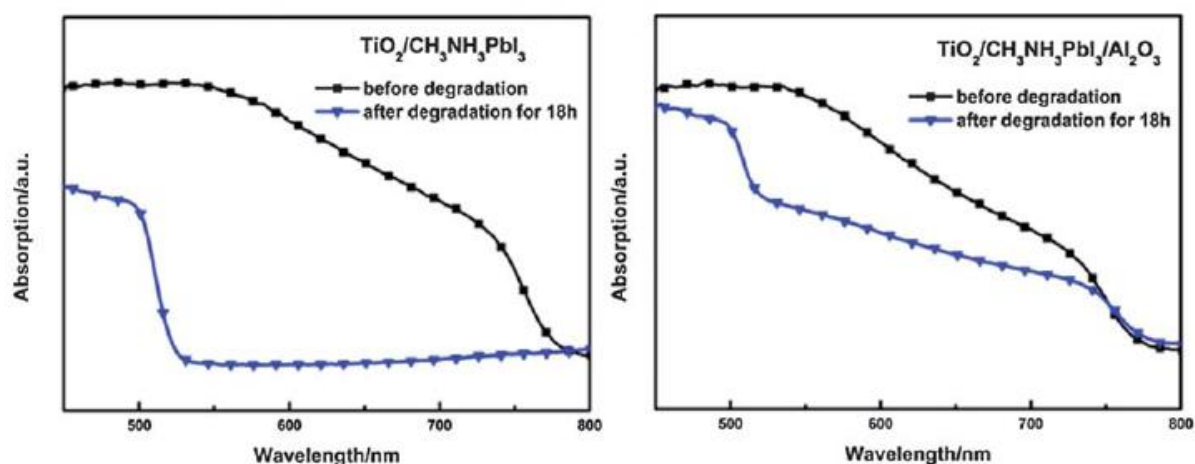
Organolead perovskite films are known to be susceptible to degradation in the presence of light and humidity². One of the by-products of degradation is lead halide. This means that for films of $\text{CH}_3\text{NH}_3\text{PbI}_3$ or $\text{CH}_3\text{NH}_3\text{PbI}_{3-x}\text{Cl}_x$ which are initially black, there is a significant colour change to the bright yellow PbI_2 during degradation. For perovskite films produced using spin coating solution-based precursors followed by sintering, *ca.* 18h is reported to be the point when light absorption reaches a minimum and the films are described as being fully degraded.

In the experiment reported here, sintered films have been kept in a sealed plastic box in the laboratory at *ca.* 40% RH. Periodically, films have been removed and monitored using diffuse reflectance UV-visible spectroscopy (DRUV-vis) to study any colour changes and typical data are shown in ESI Fig. 10a. These data show that when a film is first produced (purple line) there is intense light absorption across the visible spectrum (2.2 to 2.4 a.u. between 500-800nm) which is in line with the photographic evidence that the films are black. After exposure to 40% humidity for *ca.* 4 days, the absorption has dropped slightly to 1.7 to 1.8 a.u. which drops again to 1.5 to 1.6 a.u. after 7 days after which it remains unchanged up to 14 days. However, after *ca.* 3 months exposure to humidity (red line), the light absorption has dropped to 0.2 to 0.3 a.u. indicating that the film is almost colourless and has significantly degraded.



ESI Fig. 10a UV-visible absorption spectra of thin-film MAPbI₃ perovskite ink films.

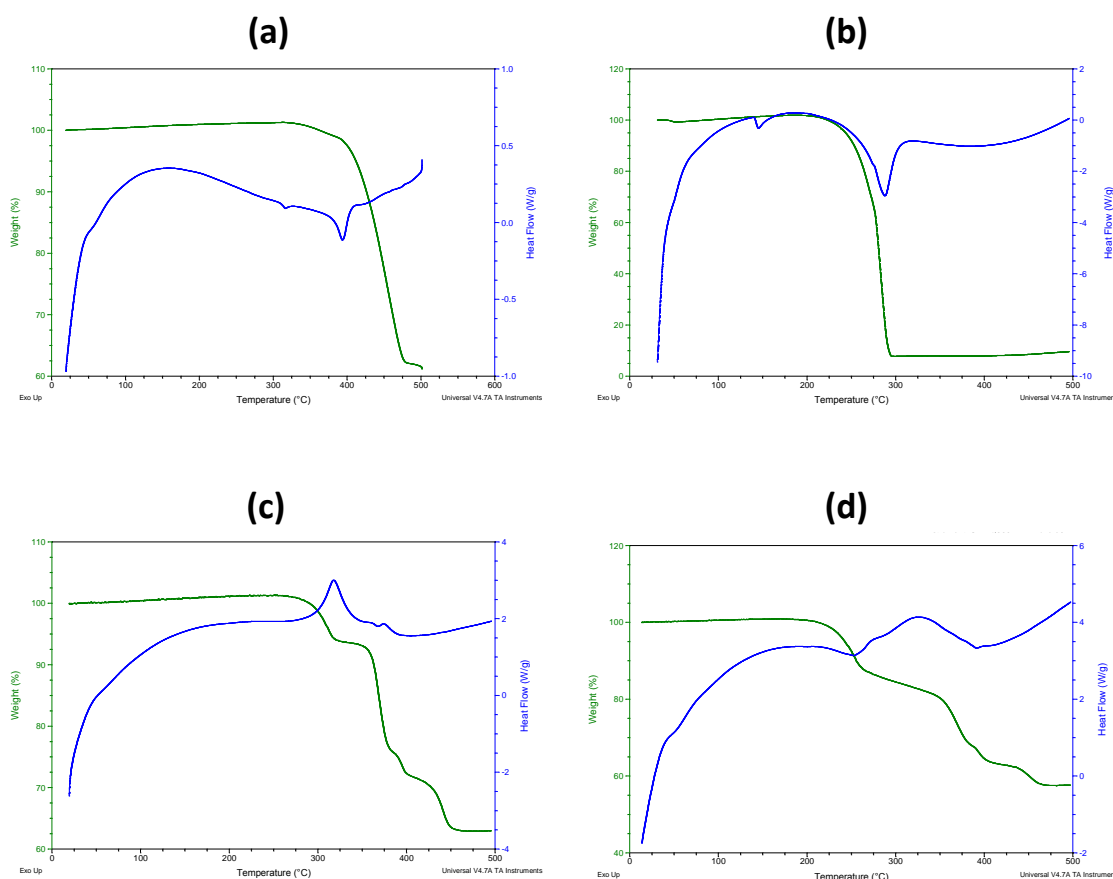
By comparison, the literature reports data for a spin coated, solution processed perovskite which shows very rapid loss of light absorption after only 24 hours (ESI Fig. 10b)³.



ESI Fig. 10b UV-visible spectra of spin coated, solution processed films (left) $\text{TiO}_2/\text{CH}_3\text{NH}_3\text{PbI}_3$ before and after 18h degradation and (right) $\text{TiO}_2/\text{CH}_3\text{NH}_3\text{PbI}_3/\text{Al}_2\text{O}_3$ before and after 18h degradation. Taken from reference³.

6.0 Thermal Analysis

ESI Fig. 11 shows thermal analysis data for the raw materials, the PbI_2 :alumina mixture and the $\text{CH}_3\text{NH}_3\text{PbI}_3/\text{Al}_2\text{O}_3$ perovskite. The lead iodide decomposes above 350°C whilst the $\text{CH}_3\text{NH}_3\text{I}$ shows a small endotherm at *ca.* 145°C which corresponds to its melting point. It then decomposes above 200°C . The data for the material produced by grinding PbI_2 and alumina (ESI Fig. 11c) shows a steep weight loss just below 400°C which is ascribed to PbI_2 on the alumina surface. The data for $\text{PbI}_2 + \text{CH}_3\text{NH}_3\text{I} + \text{Al}_2\text{O}_3$ (ESI Fig. 11d) shows that this material is thermally stable until 200°C with no mass loss incurred prior to this temperature. This means this perovskite material is thermally stable across the full range of processing temperatures used.

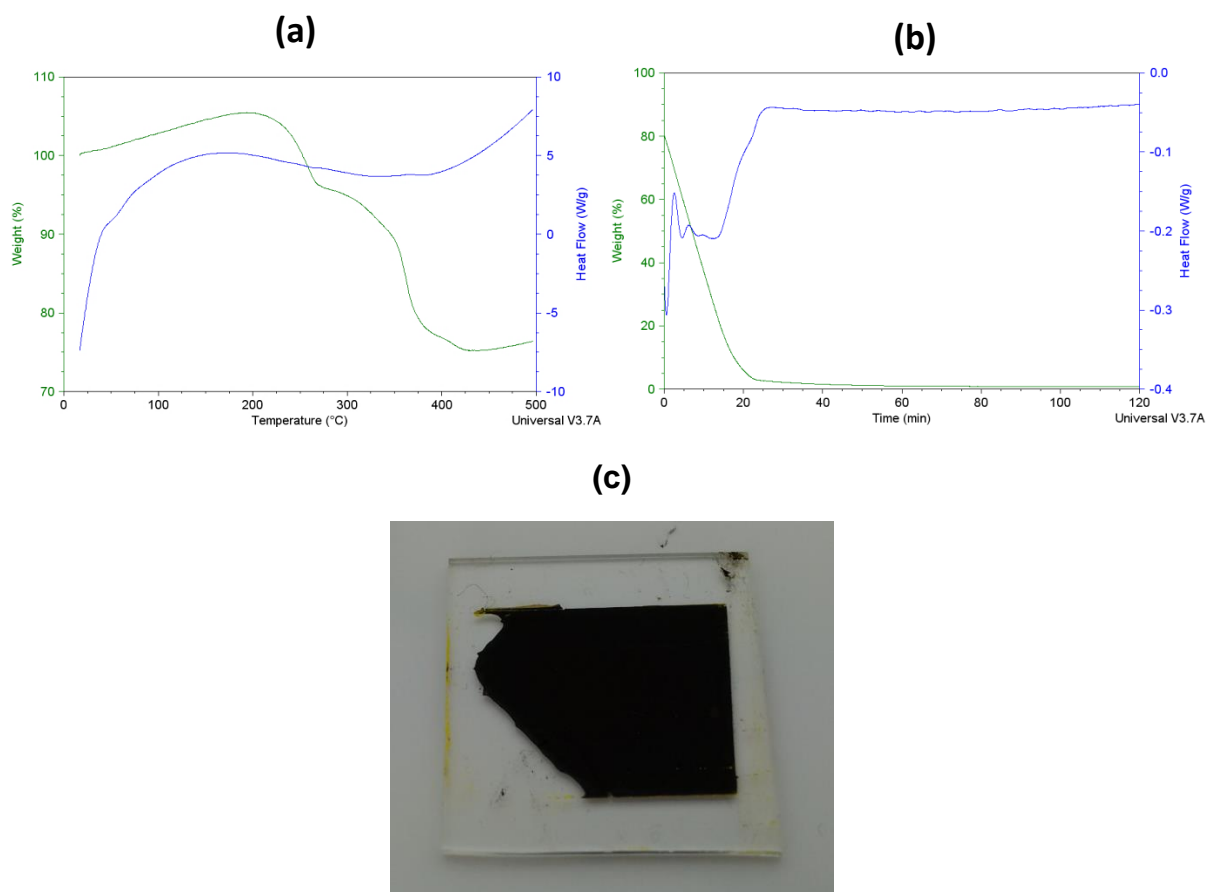


ESI Fig. 11 Thermal analysis data (TGA/DSC) for (a) PbI_2 powder, (b) $\text{CH}_3\text{NH}_3\text{I}$, (c) $\text{PbI}_2 + \text{Al}_2\text{O}_3$ and (d) $\text{PbI}_2 + \text{Al}_2\text{O}_3 + \text{CH}_3\text{NH}_3\text{I}$

6.1 Remaining Terpeneol

ESI Fig. 12 shows thermal analysis data of terpeneol-containing perovskite inks. ESI Fig. 12a shows data for a perovskite ink film which had been bar coated onto glass, heated to 120°C and then scraped off before thermal analysis. The data are very similar to ESI Fig. 11d which suggests that the weight losses are due to the organolead halide perovskite rather than terpeneol. This assignment is supported by ESI Fig. 12b which shows the result of isothermally heating neat terpeneol at 90°C . The data shows that *ca.* 20min is sufficient to remove a sample containing only terpeneol. To put this in context, the perovskite inks contain up to *ca.* 50% terpeneol and they are also heated to a higher temperature for longer; i.e. typically 50 min at 120°C .

Fig. 12c shows an image of a film deposited from a $\text{CH}_3\text{NH}_3\text{PbI}_3:\text{Al}_2\text{O}_3$ ink which has been heated to $> 200^\circ\text{C}$ to completely remove terpeneol solvent. After this, the film has been aged for 1 month in air (%RH $> 50\%$). The film remains black. These data show that the improved stability of the perovskite ink films is not due to them being coated by excess terpeneol.

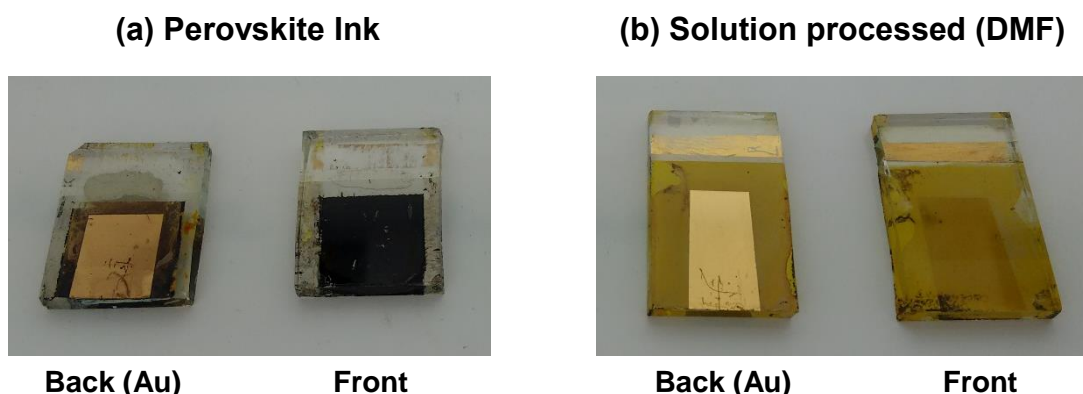


ESI Fig. 12 Thermal analysis data (TGA/DSC) for (a) post heated $\text{CH}_3\text{NH}_3\text{PbI}_3$ perovskite powder, (b) isothermal (90°C) heated terpeneol sample and (c) a film produced from $\text{CH}_3\text{NH}_3\text{PbI}_3:\text{Al}_2\text{O}_3$ ink which has been heated to $> 200^{\circ}\text{C}$ to completely remove terpeneol and then aged for 1 month in air (%RH $> 50\%$).

7.0 Planar Perovskite devices

PV devices were prepared on compact TiO_2 layers deposited on TEC15 glass. Solution processed perovskite ($\text{CH}_3\text{NH}_3\text{PbI}_3$) was spin coated from a 40% wt DMF perovskite precursor solution onto the TiO_2 layer followed by spiro-OMeTAD as a hole conduction material (HTM) as previously reported⁴. Gold (*ca.* 100nm) was evaporated onto the HTM to form a back contact. Perovskite ink ($\text{CH}_3\text{NH}_3\text{PbI}_3:\text{Al}_2\text{O}_3$) for these devices was prepared using 1.00g PbCl_2 1.68g $\text{CH}_3\text{NH}_3\text{I}$, 4.0ml terpeneol and 0.10g Al_2O_3 . The ink was also deposited onto TEC15 glass by doctor blading, the HTM was spin coated onto this and the device contacted with gold as described above. The IV characteristics of the devices were measured at 1 Sun and then the devices were allowed to age in air for 1 month (%RH $> 50\%$) before the devices were imaged (ESI Fig. 13) and the IV characteristics were re-measured (ESI Table 1). The data show that the perovskite ink devices remain black even after 1 month exposure to air. By comparison, the solution processed film has become pale yellow. The perovskite ink IV data show that, whilst these devices have not yet been fully optimised so that they are generating small J_{sc} and η is only *ca.* 1.0%, they actually improve very slightly after 24 h ageing in air to $\eta = 1.5\%$. This

is probably due to the spiro-OMeTAD oxidizing with time which improves the device fill factors by reducing series resistance. These perovskite ink devices also show higher dark current than expected and we ascribe this to unoptimised perovskite coverage leading to increased numbers of micro-junctions in the perovskite:Al₂O₃ film. However, our data do also show that perovskite ink devices still generate a small photo-current even after 1 month exposure to air whilst the solution processed device produces no measurable IV data. The scratches on the devices (ESI Fig. 13) were produced by using crocodile clips to contact onto the devices during IV measurements.



ESI Fig. 13 Perovskite ink and solution processed devices after 1 month exposure to air

ESI Table 1 IV data of solution processed CH₃NH₃PbI₃ or CH₃NH₃PbI₃:Al₂O₃ perovskite ink devices with time. Devices are all 0.12-0.25 cm² active area unless stated.

Device	Time	η / %	V_{oc} / V	I_{sc} / mA cm ⁻²	FF
Perovskite ink	As made (light)	0.9	0.81	4.20	0.27
	As made (dark)	0.4	0.75	1.14	0.44
	As made	1.1	0.96	2.44	0.45
	After 24h	1.5	0.98	2.81	0.55
	As made	1.1	0.85	2.53	0.50
	After 24h	1.5	0.94	2.44	0.63
	As made [†]	0.9	0.81	4.20	0.27
	Aged for 1 month	0.1	0.65	0.51	0.26
Solution processed	As made [‡]	5.2	0.83	12.23	0.51
	Aged for 1 month [*]	0.0	N.R.	N.R.	N.R.

[†] The back contact for this device was a PEDOT:PSS coated Ni-grid laminate⁵. All other devices were measured using a gold back contact.

[‡] Smaller device (0.023cm²)

^{*} After 1 month, the solution processed perovskite (ESI Fig. 13b) gave no result (N.R.) because the device did not work at all.

References

1. N. Noel, S.D. Stranks, A. Abate, C. Wehrenfennig, S. Guarnera, A.-A. Haghighirad, A. Sadhanala, G.E. Eperon, S.K. Pathak, M.B. Johnston, A. Petrozza, L.M. Herz, H.J. Snaith, *Energy Environ. Sci.*, 2014, **7**, 3061.
2. J. Yang, B. D. Siempelkamp, D. Liu and T. L. Kelly, *ACS Nano*, 2015, **9**(2), 1955.
3. G. Niu, W. Li, F. Meng, L. Wang, H. Dong, Y. Qiu, *J. Mater. Chem. A*, 2014, **2**, 705.
4. M.M. Lee, J. Teuscher, T. Miyasaka, T.N. Murakami, H.J. Snaith, *Science*, 2012, **338**, 643.
5. D. Bryant, P. Greenwood, J. Troughton, M. Wijdekop, M. Carnie, M. Davies, K. Wojciechowski, H.J. Snaith, T. Watson, D. Worsley, *Adv. Mater.*, 2014, **26**, 7499.

Acknowledgements

We would like to gratefully acknowledge funding from the Welsh Government for Sêr Cymru (EWJ, PJH, RJH, RA), EPSRC SPACE-modules, EP/M015254/1 (AC), EPSRC/InnovateUK SPECIFIC, EP/I019278/1 (SG), EPSRC CASE and Tata Steel (LF), EPSRC Supersolar, EP/5017361/1 (JB), the Biocomposites Centre at Bangor University for access to the SEM and NSG for supply of TEC™ glass and the Advanced Imaging of Materials (AIM) facility for high resolution electron microscopy.